TWO-STREAM PROBLEMS IN ACCELERATORS

F. Zimmermann and G. Rumolo, CERN, Geneva, Switzerland

Abstract

Electron beams are perturbed by positively charged ions in a similar way as proton and positron beams may be affected by electrons which are generated via gas ionization, photoemission, or multipacting. In particular, the ions or electrons can induce fast instabilities. These instabilities become more severe in accelerators operating with high current or close bunch spacing. They might even affect less intense muon beams during ionization cooling. Theories, simulations and observations of two-stream instabilities between a charged particle beam and either ions or electrons are reviewed.

1 INTRODUCTION

As the vacuum-chamber designs are optimized and the impedances reduced by orders of magnitude compared with earlier accelerators, two-stream effects may pose new limitations on the beam current. Namely the interaction of a charged particle beam with a second particle species, usually of opposite charge, can result in emittance growth or instability. In electron storage rings, the most prominent interacting particle species are ions, whereas in positron and proton rings the primary concern are electrons generated by photoemission, multipacting, or ionization. The next section reviews classical and fast ion instabilities. Section 3 addresses electron-cloud effects, including electron-driven single and coupled-bunch instabilities. We conclude with a short summary. SI units are used throughout.

2 ION EFFECTS

A charged particle beam ionizes the residual gas, producing ions at a rate

$$\dot{\lambda}_{\text{ion}}[\text{m}^{-1}\text{s}^{-1}] = (I_{\text{beam}}/q)\sigma_{\text{ion}}d_{\text{gas}} \qquad (1)$$

where d_{gas} is the molecule density in m^{-3}, λ_{ion} the ion line density in m^{-1}, I_{beam} the beam current, and q the beam-particle charge. At relativistic energies the ionization cross section σ_{ion} is about 2 Mbarn, for carbon monoxide. The ion accumulation saturates when ion losses balance the generation, *e.g.*, either due to beam neutralization, or due to multiple ionization and loss of the ions with higher charge. In the second case, the asymptotic value of the ion density is comparable to the residual gas density. If the beam is negatively charged (electron, antiproton or H^- beams), the ionization electrons are rapidly repelled towards the wall, whereas the ions accumulate in the beam potential. The ion space charge field then induces coherent and incoherent tune shifts.

Near the beam axis the transverse restoring force on the ions is linear. If the beam is bunched and the gap between successive bunches is large, ions are overfocused and escape from the beam potential. Ions are trapped by the bunch train only, if their mass A (in units of the proton mass m_p) exceeds a critical value A_{crit}. Considering a beam of N_e electrons stored in a ring of circumference C and consisting of n_b uniformly distributed bunches with transverse rms beam sizes $\sigma_y < \sigma_x$, the critical mass is [1]

$$A_{\text{crit}} = \frac{N_e C r_p Q}{n_b^2 2\sigma_y(\sigma_x + \sigma_y)}, \qquad (2)$$

where r_p denotes the classical proton radius, and Q the ion charge in units of the electron charge e. The trapped ions perform transverse oscillations around the beam center, with horizontal and vertical angular frequencies

$$\omega_{i;x,y} \approx \left(\frac{2N_e r_p Q c^2}{C\sigma_{x,y}(\sigma_x + \sigma_y)A} \right)^{1/2}, \qquad (3)$$

where c denotes the speed of light. In electron rings, the vertical rms beam size σ_y is usually smaller than the horizontal rms size σ_x, and, therefore, the vertical ion frequency is higher than the horizontal one. An ion frequency spread is introduced (1) by the beam-size variation around the ring and (2) by the nonlinearity of the beam field at larger amplitudes.

For coasting beams, as well as for bunched beams with close spacing and $A > A_{\text{crit}}$, ions are trapped over multiple turns. Then a classical beam-ion instability can develop, *i.e.*, a resonantly coupled growing oscillation of the beam and ion motion. Such instabilities have been observed and studied at many accelerators [2]–[13]. The instability can arise if

$$\omega_\beta + m\omega_0 \approx \omega_i \qquad (4)$$

where ω_β is the (fractional) betatron frequency, ω_0 the revolution frequency, and m an integer. Since the size of the ion cloud is comparable to the beam size, the coefficient

$$K_{x,y} = \frac{2\lambda_{\text{ion}}r_e c^2}{\gamma\sigma_{x,y}(\sigma_x + \sigma_y)}, \qquad (5)$$

characterizes the focusing of the beam by the ions. The growth rate of the classical ion instability is [10, 14]

$$\frac{1}{\tau_{\text{trap}}} = \frac{K}{2\omega_\beta} \left[\frac{\pi}{2}\omega_R \rho_i(\omega_R) \right], \qquad (6)$$

where $\omega_R \approx \omega_\beta + m\omega_0$ denotes the frequency of the unstable mode and ρ_i the normalized ion frequency distribution. We have dropped the subscripts x, y. In damping

rings for future linear colliders, the beam sizes decrease strongly during the store time (10–100 ms) and, thus, the ion frequencies (3) increase. Once the resonance condition (4) is met, an instability occurs, where beam motion is excited in short bursts, by which either the ions are expelled from the beam potential or the beam size is blown up. Resonances are encountered for different ion species at various times during the store. An ion instability of this type has been observed at the SLC damping ring [11].

The ion instabilities may be suppressed by radiation damping, head-tail damping, transverse feedback, or by a betatron frequency spread that exceeds the ion-induced betatron frequency shift $\Delta\omega_\beta \approx K/(2\omega_\beta)$. In small rings, it can also happen that at moderate currents the frequency corresponding to the fractional part of the betatron tune is higher than the ion oscillation frequency, in which case there is no instability. However, the standard approach of avoiding trapped ion instabilities in a storage ring is the introduction of a large clearing gap of missing bunches. The required gap length is $t_{\text{gap}} \gg 2/\omega_i$.

If a clearing gap removes the ions, the maximum number of ions is limited to those produced during a single passage of the bunch train. Unfortunately, modern factories and future collider projects require much higher beam current than previous storage rings, and the ion production rate (1) increases correspondingly. In addition, high-quality beams are characterized by smaller beam sizes, which enhances the coupling between the beam and the ions, described in Eqs. (3) and (5). Therefore, an ion instability can occur even in the presence of a clearing gap. This transient instability is similar to multi-bunch beam break up in a linac and it has been called the 'fast beam-ion instability' (FBII) [15, 16, 17]. In this case, the coupling (5) is not a constant but, due to the ion production, it increases linearly along the bunch train. We write $K = \dot{K}z/c$ where z denotes the distance from the head of the bunch train (we assume that the beam is relativistic), and, using $\dot{\lambda}_{\text{ion}}$ from (1),

$$\dot{K}_{x,y} = \frac{2\dot{\lambda}_{\text{ion}} r_e c^2}{\gamma\sigma_{x,y}(\sigma_x + \sigma_y)}. \qquad (7)$$

Without ion frequency spread, the bunch oscillation amplitudes grow as

$$y_b(s,z) \propto \exp\left(\sqrt{\frac{s}{c\tau_{\text{FBII}}}\frac{z}{l_{\text{train}}}}\right), \qquad (8)$$

where s denotes the position along the beam line, l_{train} the length of the bunch train, and the quasi-exponential instability rise time at the end of the bunch train ($z = l_{\text{train}}$) is [15, 16, 18]

$$\tau_{\text{FBII}} = \sqrt{\frac{2\omega_\beta c^2}{\dot{K}_{\text{ion}}\bar{\omega}_i l_{\text{train}}}}. \qquad (9)$$

Inserting the definitions, and taking into account that the ion centroid frequency $\bar{\omega}_i$ is about $\sqrt{2/3}$ of ω_i (3), the growth rate can also be written as [15]

$$\frac{1}{\tau_{\text{FBII}}} = \frac{4d_{\text{gas}}\sigma_{\text{ion}}\beta_y N_b^2 r_e^{3/2} n_b^2 L_{\text{sep}}^{1/2} c}{\sqrt{27}\gamma\sigma_y^{3/2}(\sigma_x + \sigma_y)^{3/2}A^{1/2}}, \qquad (10)$$

where $N_b = N_e/n_b$ is the bunch population, and L_{sep} the bunch spacing (in m). Equation (9) is valid for [18, 19, 20]

$$\dot{K}l_{\text{train}}^2\bar{\omega}_i/(8\omega_\beta^3 c) \ll s \ll 2\bar{\omega}_i\omega_\beta c/\dot{K}, \qquad (11)$$

which is almost always fulfilled [20]. The limit on the right-hand side of Eq. (11) arises from the ion-induced tune shift. If s exceeds this limit, the instability saturates due to BNS damping [21]. At this point, the initial perturbation has increased by a factor $\exp(\bar{\omega}l_{\text{train}}/c)$ [20, 18], which typically amounts to a huge factor of 10^{10}–10^{20}.

Much earlier, however, the instability slows down due to other mechanisms: The growth of unstable oscillations ceases at amplitudes comparable to the rms beam size, since here the beam-ion force becomes strongly nonlinear [22]. In addition, variation of the beam sizes around the ring, the presence of multiple ion species, the dependence of the vertical ion frequency on the horizontal position, as well as the nonlinearity of the beam field, all introduce a spread in the effective ion frequency. This ion frequency spread qualitatively changes the character of the instability, such that it becomes truly exponential [17, 18]. For a normal distribution of ion frequencies, with mean $\bar{\omega}_i$ and standard deviation σ_ω, the amplitude grows as

$$y_b(s,z) \propto \exp\left(\frac{s}{c\tau_{\text{FBII2}}}\frac{z}{l_{\text{train}}}\right) \qquad (12)$$

where

$$\tau_{\text{FBII2}} = \frac{2\omega_\beta c}{\dot{K}l_{\text{train}}}\left[\sqrt{\frac{8}{\pi}}\frac{\sigma_\omega}{\bar{\omega}_i}\right] \qquad (13)$$

If the ion distribution is broad, $\sigma_\omega \approx \bar{\omega}_i$, the instability growth rate equals the incoherent betatron frequency shift induced by the ions $1/\tau_{\text{FBII2}} \approx \Delta\omega_\beta \approx (2\omega_\beta c/(\dot{K}l_{\text{train}}))$ [18]. This is reminiscent of the result for the trapped-ion instability with frequency spread (6). Solution (12) is valid for $s \ll 2\sigma_\omega\omega_\beta c/\dot{K}$ [18]. At $s \approx 2\sigma_\omega\omega_\beta c/\dot{K}$ an initial perturbation has been amplified by the same factor $\exp(\bar{\omega}_i l_{\text{train}}/c)$ as for $\sigma_\omega = 0$, *i.e.*, the amplification is independent of the ion frequency spread.

Experimentally, the fast beam-ion instability has first been observed at the Advanced Light Source [23], the TRISTAN AR [24], and the Pohang Light Source [25, 26]. In most experiments, the vacuum pressure was intentionally degraded by venting with He gas to 5–80 nTorr. Even in the presence of large clearing gaps, an ion instability was observed. Evidence included excitation of betatron sidebands near the estimated ion frequency which varies with the vertical beam size, oscillations or emittance growth increasing from the head to the tail of the bunch train, and, unambiguously, direct observation using a streak camera [26]. These experiments also demonstrated that short gaps in the bunch train, the presence of different ion species, or enlarged chromaticity may damp the instability [26, 27]. More recently, the instability has been observed in the KEKB HER during commissioning [28]. The KEKB analysis applied a singular-value decomposition [29] to multi-turn bunch-by-bunch BPM data [28]. A fit to the growth

rate was roughly consistent with the theoretical prediction. Lately, the instability has been seen at the ESRF when operating with a low-emittance lattice and poor vacuum [30], and at SPring-8 [31].

Single-pass emittance dilution due to ions also occurs for single bunches at locations with nonzero dispersion, if energy and longitudinal position are correlated [32].

3 ELECTRON CLOUD

Positively charged beams preferably interact with electrons, which can be trapped in their potential well, just as ions are attracted by beams of negative charge. The electrons oscillate inside a single bunch of rms length σ_z with the approximate frequency

$$\omega_{e;x,y} \approx c \left(\frac{2N_b r_e}{\sqrt{2\pi}\sigma_z \sigma_{x,y}(\sigma_x + \sigma_y)} \right)^{1/2}. \qquad (14)$$

The electron oscillation frequency ω_e is much larger than ω_i, due to the large mass difference of ions and electrons. Electrons can thus more easily induce single-bunch instabilities, in addition to coupled-bunch instabilities.

In most proton rings, the dominant source of electrons is gas ionization, in most positron rings it is synchrotron radiation and photoemission. In either case, for close bunch spacing beam-induced multipacting can further amplify the number of electrons by a significant factor. A necessary condition for the electron amplification is that the average secondary emission yield exceeds 1. The latter depends on the energy gained by electrons in the beam field, and, hence, on the bunch current, the bunch length, and the chamber dimension. The secondary electrons consist of both true secondaries and elastically scattered or rediffused electrons. Parametrizations can be found in Refs. [33, 34, 35, 36]. True multipacting occurs if electrons emitted from the surface reach the opposite chamber wall exactly at the moment the next bunch passes by, so that the newly produced secondaries are again accelerated in the beam field, *i.e.*, if [37]

$$n_{\min} \equiv h_y^2 / (N_b r_e L_{\text{sep}}) = 1, \qquad (15)$$

where h_x and h_y are the chamber half apertures. For $n_{\min} < 1$, part of the primary electrons are lost before the next bunch arrives, leaving behind low-energetic secondaries. For $n_{\min} > 1$, the primary electrons interact with more than 1 bunch. Electron amplification is observed for a large range of $n_{\min}$ values, not only for $n_{\min} \approx 1$ [38].

The electron build up saturates when the attractive beam field is on average compensated by the field of the electrons. The saturated electron line density λ_{el} is roughly

$$\lambda_{\text{el,neutr}} = N_b / L_{\text{sep}}, \qquad (16)$$

where the electron field on average compensates the beam field, at the chamber wall. Assuming a uniform distribution, $\lambda_{\text{el,neutr}}$ corresponds to a volume density

$$\rho_{\text{el,neutr}} \approx \lambda_{\text{el,neutr}} / (\pi h_x h_y). \qquad (17)$$

The electron cloud can link together the motion of subsequent bunches and induce a coupled-bunch (CB) instability [39, 40], because bunches which are off-set transversely will perturb the electron-cloud distribution and, thereby, also the following bunches. Consider a bunch transversely off-set by Δy which traverses a stationary electron cloud. Over a beam-line section of length l_b the following bunch receives a deflection $\Delta y'$ from the disturbed electron cloud, which is related to the bunch-to-bunch dipole wake field per unit length, in units of m^{-3}, through

$$\left(\frac{W_{1,y}}{L} \right)_{\text{e,CB}} = \frac{\Delta y'}{\Delta y} \frac{\gamma}{r_p N_b l_b}, \qquad (18)$$

and, thereby, to the instability rise time [35, 41]

$$\tau_{\text{e,CB}} \approx \frac{2\gamma\omega_\beta}{N_b r_p c^2 (W_{1,y}/L)_{\text{e,CB}}}. \qquad (19)$$

Approximating the wake field as $(W_{1,y}/L)_{\text{e,CB}} \approx 4\pi\rho_{\text{el}}/N_b$, and assuming $\rho_{\text{el}} \approx \rho_{\text{el,neutr}}$ (17), the rise time of Eq. (19) becomes

$$\tau_{\text{e,CB}} \approx \frac{\gamma\omega_\beta}{2\pi r_p c^2 \rho_{\text{el}}} \approx \frac{\gamma\omega_\beta h_x h_y L_{\text{sep}}}{2r_p N_b c^2}. \qquad (20)$$

The electron cloud also drives a single-bunch (SB) instability, which potentially appears more dangerous than the coupled bunch instability, since it cannot easily be damped by a feedback system. The single-bunch wake field and the associated instability threshold may be estimated from a two particle model [42], where the bunch consists of a head and tail particle, each carrying the charge $N_b e/2$. Unlike an ordinary wake field, a finite length, $\sim \sigma_z$, must be assigned to the leading particle, since the electron motion depends on the beam density. Then, for sufficiently long bunches, *i.e.*, for $\sigma_z \omega_e > c\pi/2$, the wake field acting on the trailing particle (in units of m^{-2}) is [42]

$$W_{y,\text{SB}} \approx 8\pi\rho_e C/N_b, \qquad (21)$$

and comparable to our estimate for the coupled-bunch wake field. Note that the electron density increases roughly in proportion to the population of the (preceding) bunches, $\rho_e \propto N_b$, so that, for equally intense bunches, $W_{y,0}$ is independent of N_b like a regular wake field. For example, assuming that the electron density equals the neutralization density (17), $\rho_{\text{e,sat}} \approx \rho_{\text{e,neutr}}$, the wake field is

$$W_{y,\text{SB}} \approx \frac{8C}{L_{\text{sep}} h_x h_y}, \qquad (22)$$

which depends only on geometric quantities. In a ring with synchrotron oscillations, the instability manifests itself as a strong head-tail or transverse mode-coupling instability (TMCI). Using (21) the threshold electron density for the TMCI is [42]

$$\rho_{\text{e,thr}} \approx \frac{2\gamma Q_s}{\pi\beta_y r_p C} \qquad (23)$$

where T_0 is the revolution period, and Q_s the synchrotron tune. Since $\rho_{e,neutr} \propto N_b/L_{sep}$, this implies the scaling $N_{b,thr} \propto L_{sep}$, possibly consistent with KEKB observations [43]. For many future or present accelerators, *e.g.*, PEP-II, KEKB, LHC, SPS, PSR, or SNS, the neutralization density, (17) and (16), exceeds the threshold (23) [38].

Beam instabilities due to electrons were first observed with coasting proton beams or long single proton bunches in Novosibirsk [44, 45], the CERN ISR [46], and at the Los Alamos PSR [47]. Beam-induced multipacting was seen already at the ISR, in bunched beam operation [48]. The first observation of a coupled-bunch electron-cloud instabilities for a positron beam was made at the KEK Photon Factory [39, 40]. The effect was reproduced in BEPC [49]. Thereafter, studies were launched for the PEP-II B factory [50, 51], and LHC [41, 37, 52, 53, 54, 55, 56]. A similar instability at CESR was caused by electrons trapped in the leakage field of the ions pumps [57]. Since 1998, electron-cloud effects are seen with the LHC proton beam in the SPS [58], and since 2000 in the CERN PS prior to beam extraction, and in the PS-to-SPS transfer line [59]. The SPS observations include beam loss and emittance growth, and evidence for coupled-bunch motion in the horizontal plane and for a single-bunch instability in the vertical. Electron clouds are also responsible for beam-size blow up and luminosity limitations observed in the two positron rings of PEP-II [60] and KEKB [43, 61, 62], though they appear to be absent in Dafne, which is not fully understood [63]. Since, unlike the case of the photon factory, the B factories do not show coupled bunch oscillations, the beam blow up must be due to a single-bunch instability. At KEKB this was confirmed by a witness bunch experiment [61]. At the SPS, the motion inside individual bunches was detected with a broadband pick up, and fitted to a wake-field of frequency $\sim \omega_e$ [64].

Various simulation codes model the build up of the electron cloud in the vacuum chamber [40, 35, 41], the wake field and the single-bunch instability [42, 65, 66, 67, 68]. Figure 1 displays the simulated transverse wake field for a Gaussian beam profile [69]. Since the electron density and oscillation frequency ω_e vary along the bunch, this wake field depends on the source point, unlike a regular wake.

The electron cloud can also give rise to incoherent effects, *e.g.*, at KEKB an incoherent tune spread of $\Delta Q_y \approx 0.03$ is observed (3–5 times the coherent tune shift) [62, 38]. This is explained by the accumulation of electrons near the beam axis during the passage of a bunch [70]. The local increase in the electron density by about a factor of 10 causes a tune difference between bunch head and tail.

For lower-energy proton beams an additional tune variation along the bunch arises from the beam space charge. Recent PIC simulations suggest that adding the proton space-charge to the electron cloud qualitatively changes the character of the single-bunch instability [69]. In the presence of space charge a violent centroid motion develops along the bunch, whereas with the electron cloud only a fast but calm increase in the beam size prevails. This is il-
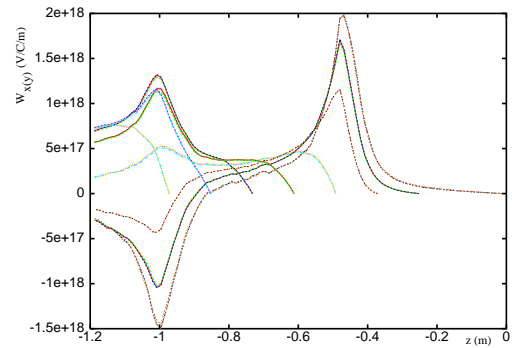

Figure 1: Simulated vertical wake field in V/m/C, excited by displacing various slices inside the Gaussian bunch, vs. position in m, for an SPS field-free region. The bunch center is at -0.6 m, the bunch head ($2\sigma_z$) on the right.

lustrated in Fig. 2. In the simulation, the space charge force damps regular impedance-driven instabilities.
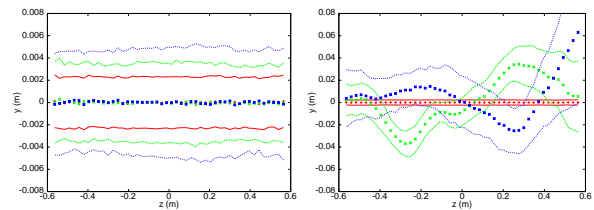

Figure 2: Simulated vertical bunch shape (centroid and rms beam size) after 0, 250, and 500 turns in the CERN SPS assuming an electron cloud density $\rho_e = 10^{12}$ m^{-3} without (left) and with (right) proton space charge at 26 GeV/c.

For the LHC and any future hadron collider employing superconducting magnets, a further concern is the electron-cloud heat load on the cryogenic system. The electron energy incident on the chamber wall can widely exceed the heat deposited by proton synchrotron radiation. Special chamber preparations and commissioning recipes are foreseen to stay within tolerable limits. The surface conditioning, *i.e.*, the decrease of the secondary emission yield as a function of accumulated dose will play a central role.

An electron wake field also arises during the interaction of a high-current electron beam and an antiproton bunch in the FNAL Tevatron electron lens, where the resulting TMCI instability is suppressed by a longitudinal solenoid field of a few T [71]. A similar situation is encountered in the ionization cooling cells of a neutrino factory or muon collider [72]. These cells contain liquid hydrogen at cryogenic temperature in a strong solenoid of field B. Electrons and ions are produced by ionization. The electrons rotate at the Larmor frequency $\omega_L = eB/m_e$. If a slice or bunch of the beam is horizontally offset by Δx it will induce a horizontal and a vertical (skew) wake. Using again a two particle model, the skew wake field [71] excited by

the (pointlike) head of charge $N_b e/2$, in units of m^{-2}, is

$$W_{1,\mathrm{icool}} \approx \frac{\sigma_{\mathrm{ion}} d_{H_2} N_b L_{\mathrm{cell}}}{8\pi\sigma_r^4} \left[\frac{Z_0}{B/e}\right] \qquad (24)$$

where L_{cell} is the total length of the liquid hydrogen cells, d_{H_2} is the hydrogen volume density, Z_0 the vacuum impedance, σ_{ion} the ionization cross section for 200 MeV muons, and σ_r the rms transverse beam size. An initial perturbation grows by a factor

$$A_{\mathrm{icool}} \approx r_\mu \beta_\mu N_b W_{1,\mathrm{icool}}/(4\gamma_\mu) \qquad (25)$$

where β_μ is the muon beta function, and r_μ the classical muon radius. For a neutrino factory, the factor is less than 1, but for a future muon collider [73] it can be significant. Whether the preceding estimate is indeed appropriate for electrons in liquid hydrogen at cryogenic temperature still remains to be studied. For example, immediate recombination of most electrons and limited electron mobility [74] might considerably reduce the estimate (25).

Finally, synergy between ions and electrons is unlikely to occur. The number of ions and their survival time are far too low to influence the electron cloud [75].

4 CONCLUSIONS

The performance of many present and future accelerators is limited by two-stream instabilities, developing between the beam and either ions or electrons. New types of effects emerge as the beam currents increase, and bunch spacings or emittances decrease. A theoretical framework is available to describe these effects and to infer possible cures.

5 ACKNOWLEDGMENTS

6 REFERENCES

[1] Y. Baconnier, G. Brianti, CERN/SPS/80-2 (DI) (1980).
[2] G.I. Budker, Sov. Atomic Energy 5, 9 (1965).
[3] B.V. Chirikov, Sov. Atomic Energy 19, p. 239 (1965).
[4] E. Keil and B. Zotter, CERN ISR-TH/71-58 (1971).
[5] G. Koshkarev and P. Zenkevich, Part. Acc. 3, 1 (1972).
[6] L.J. Laslett et al., Nucl. Instr. Meth. A 121, 517 (1974).
[7] E. Jones et al., 1985 IEEE PAC, New York, p. 2218 (1985).
[8] S. Sakanaka et al., NIM A 256, p. 184 (1987)
[9] A. Poncet, in Frontiers of Particle Beams: Intensity Limitations, Lect. Notes Phys. Vol. 400, Springer Verlag (1990).
[10] D. Sagan, A. Temnykh, Nucl. Instr. Meth. A 344, 459 (1994).
[11] P. Krejcik, PAC 97 Vancouver (1997).
[12] J.C. Lee et al., IEEE PAC 99, New York (1999).
[13] M. Popovic et al., 8th ICFA workshop, Santa Fe (2000).
[14] R.A. Bosch, subm. to Nucl. Instr. Meth. A (1998).
[15] T. Raubenheimer, F. Zimmermann, Phys. Rev. E 52, 5, p. 5487 (1995).
[16] G.V. Stupakov et al., Phys. Rev. E 52, 5, p. 5499 (1995).
[17] G.V Stupakov, Proc. CEIBA'95, KEK 96-6 (1996).
[18] R.A. Bosch, PRST-AB 3, 034402 (2000).
[19] D. Pestrikov, PRST-AB 2, 044403 (1999).
[20] G. Stupakov, PRST-AB 3, 019401 (2000).
[21] V.E. Balakin et al., 12th Int. Conf. High Energy Acc., Batavia (1983).
[22] S. Heifets, IEEE PAC 97 Vancouver (1997).
[23] J. Byrd et al., Phys. Rev. Lett. 79, 79 (1997).
[24] H. Fukuma et al., Proc. MBI'97, KEK 97-17, p. 1 (1997).
[25] M. Kwon et al., Phys. Rev. E 57, 5, p. 6016 (1998).
[26] J Huang et al., Phys. Rev. Lett. 81, p. 4388 (1998).
[27] F. Zimmermann et al., ICFA Workshop Factories, Frascati Phys. Series X, p. 399 (1997).
[28] Y. Ohnishi et al., Proc. EPAC2000, Vienna, p. 1167 (2000).
[29] J. Irwin et al., Phys. Rev. Lett. 82, p. 1684 (1999).
[30] R. Nagaoka et al., EPAC 2000 Vienna (2000).
[31] T. Nakamura et al., PAC 2001 Chicago (2001).
[32] P. Emma et al., EPAC 94 London (1994).
[33] H. Seiler, J. Appl. Phys. 54 (11) (1983).
[34] R. Kirby et al., SLAC-PUB-8212 (2000).
[35] M.A. Furman et al., KEK Proc. 97-17, p. 170 (1997).
[36] V. Baglin et al., LHC-Project-Report-472 (2001)
[37] O. Gröbner, PAC97, Vancouver (1997).
[38] F. Zimmermann, PAC 2001 Chicago (2001).
[39] M. Izawa et al., Phys. Rev. Lett. 74, 5044 (1995).
[40] K. Ohmi, Phys. Rev. Lett. 75, 1526 (1995).
[41] F. Zimmermann, LHC PR 95, SLAC-PUB-7425 (1997).
[42] K. Ohmi, F. Zimmermann, Phys. Rev. Lett. **85**, 3821 (2000).
[43] K. Oide, Chamonix XI, CERN-SL-2000-007 DI (2001).
[44] V. Dudnikov, IEEE PAC 2001 Chicago (2001).
[45] G.I. Dimov et al., Soviet Conf. Charged Part. Acc., Moscow 1968, p. 312 (1968).
[46] H. Hereward, CERN 71-15; E. Keil, B. Zotter, CERN-ISR-TH-71-58 (1971).
[47] D. Neuffer et al., Part. Acc. 23 (1988); NIM A 321 (1992).
[48] O. Gröbner, HEACC'77, Protvino (1977).
[49] Z.Y. Guo et al., APAC 98, Tsukuba (1998).
[50] M. A. Furman et al., PAC97, Vancouver (1997).
[51] S. Heifets, SLAC-PUB-6956 (1995).
[52] O. S. Brüning, CERN LHC PR 158 and EPAC98 (1997).
[53] J.S. Berg, LHC Project Note 97 (1997).
[54] G. Stupakov, CERN LHC PR 141 (1997); L. Vos, CERN LHC PN 150 (1998).
[55] M. Furman, LHC Project Report 180 (1998).
[56] F. Zimmermann, Chamonix X & XI, CERN-SL-2000-007 & 2001-003-DI; G. Rumolo et al., PRST-AB 012801 (2001).
[57] T. Holmquist, J. Rogers, Phys. Rev. Lett. 79, 3186 (1997).
[58] G. Arduini et al., EPAC 2000 Vienna, and PAC 2001 Chicago (2001).
[59] E. Metral et al., PAC 2001 Chicago (2001).
[60] A. Fisher, HEACC'01, SLAC-PUB-8815 (2001).
[61] H. Fukuma et al., HEACC'01 Tsukuba (2001); H. Fukuma et al., EPAC2000 Vienna (2000); H. Fukuma and K. Ohmi, private communications (2001).
[62] T. Ieiri et al., HEACC01 Tsukuba (2001).
[63] M. Zobov, private communication (2001).
[64] K. Cornelis, Chamonix XI, CERN-SL-2001-003-DI.
[65] G. Rumolo et al., PAC 2001, Chicago (2001).
[66] K. Ohmi, PAC 2001, Chicago (2001).
[67] S. Lee, T. Katsouleas, private comm. (2001).
[68] Y. Cai et al., PAC 2001 Chicago (2001).
[69] G. Rumolo et al., Two-Stream Workshop KEK (2001).
[70] M.A. Furman et al., PAC99 Washington (1999).
[71] A. Burov et al., PRE 59, p. 3605 (1999).
[72] B. Autin, private communication (2001).
[73] A. Ankenbrandt et al., PRST-AB 2, 081001 (1999).
[74] N. Zessoules et al., J. Appl. Phys. 34, 7, p. 2010 (1963).
[75] G. Rumolo et al., CERN-SL-2001-014 AP (2001).